A R C H I V E S O F M E T A L L U R G Y A N D M A T E R I A L S
Volume 50 2005 Issue 1

J. JELEŃKOWSKI*, S.J. SKRZYPEK**, W. RATUSZEK**, T. WIERZCHOŃ*

NEW APPROACH TO SURFACE LAYER CHARACTERISATION AFTER MECHANICAL AND THERMO-CHEMICAL TREATMENT OF HIGH NICKEL AUSTENITIC ALLOY

NOWA CHARAKTERYSTYKA WARSTW POWIERZCHNIOWYCH PO MECHANICZNEJ I CIEPLNO-CHEMICZNEJ OBRÓBCE WYSOKONIKLOWEGO STOPU AUSTENITYCZNEGO

Various kinds of fatigue experiments, machining and surface treatments can cause a phase transformation and/or non-uniform plastic deformation in surface layers of heat-treated and stainless steels or other materials containing metastable phases. It is connected with a volume change and non-uniform elasto-plastic deformation, which create residual macro and/or micro- stresses. The phase composition and distribution of residual stresses reveal gradient-like properties in most cases. Surface preparation usually requires a treatment like grinding and/or polishing and burnishing before coat is deposited.

It was found that burnishing caused large compressive residual stresses and phase transformation of austenite in thin surface layer whereas grinding resulted in tensile surface stresses.

An application of the $g\text{–}sin^2\psi$ method based on the grazing angle X-ray diffraction geometry makes it possible to obtain the real value and also the distribution of residual macro-stresses. The incorporation of this geometry to the X-ray diffraction phase analysis enables an analysis the phase contents under the surface using non-destructive means.

Keywords: high nickel alloy, non-destructive structural examinations, surface layers, grazing incidence angle X-ray diffraction geometry, phase composition, residual macrostresses

Różnorodne eksperymenty zmęczeniowe, obróbka mechaniczna i niektóre obróbki powierzchniowe mogą wywołać przemianę fazową, niejednorodne odkształcenie sprężyste i plastyczne w warstwach powierzchniowych obrobionych cieplnie stali lub innych materiałów zawierających metastabilne fazy. Takie zjawisko jest związane z lokalną zmianą objętości, co z kolei wywołuje niejednorodne odkształcenia sprężysto-plastyczne, które wytwarzają makro i mikro-naprężenia własne. Skład fazowy i rozkład naprężeń własnych są cechami gradientowymi w tego typu przpadkach.

* WYDZIAŁ INŻYNIERII MATERIAŁOWEJ, POLITECHNIKA WARSZAWSKA, 02-507 WARSZAWA, UL. WOŁOSKA 141
** WYDZIAŁ METALURGII I INŻYNIERII MATERIAŁOWEJ, AKADEMIA GÓRNICZO-HUTNICZA, 30-059 KRAKÓW, AL. MICKIEWICZA

Badania wykazały, że nagniatanie kuleczkami spowodowało duży stan ściskających naprężeń własnych i znaczną przemianę fazową stopowego austenitu, natomiast szlifowanie wywoływało rozciągające naprężenia własne.

Zastosowanie metody $g-sin^2\psi$ opartej na dyfrakcji promieni X w geometrii stałego kąta padania (zwanej też geometrią kąta poślizgowego) umożliwiło pomiary rzeczywistych wartości gradientowego rozkładu naprężeń własnych.

Zastosowanie tej dyfrakcji do ilościowej analizy fazowej umożliwiło badania rozkładu zawartości faz wzdłuż głębokości w nieniszczący sposób.

1. Introduction

A N26MT2Nb high nickel austenitic alloy can be applied in various states of microstructure, which effect in a wide range of mechanical properties (e.g. unit strength (R_m/ρ) and toughness (K_{Ic})) [1]. Many advantages of this steel are connected with mechanical instability of austenite that means its flexibility to martensite transformation during plastic strain (TRIP effect) and its ability to internal work hardening and ageing. The nitriding process can improve the mechanical properties particularly, when nitrogen austenite can be formed without chromium-nitride compounds in the diffusion layer [4]. The preparation of such layers involves low temperature of nitriding, which considerably elongates the process. Time and temperature of the nitriding can be reduced using electro-spark nitriding of the alloy with a strain induced martensite layer, prior to nitriding [4]. That is due to larger diffusion coefficient of N in the α phase. Probably the tensile/compression micro-fields between α/γ grains can also enhance the diffusion of nitrogen.

When this steel is purely austenitic (used in nuclear power engineering or space technology) or austenitic-martensitic (for constructional elements and tools), especially when it is not hardened it exhibits similarity to 18-8 austenitic steel [2]. Its advantage, in comparison with some classical austenitic steel, is a good intercrystalline corrosion resistance, especially when the microstructure of the alloy appears as duplex steel or, when this steel has a mixed nanocrystalline and microcrystalline morphology. Mechanical properties of this steel can be improved to a large extent by the nitriding process [1, 3].

The aim of this research was to examine the phase composition and residual macroscopic stresses in the surface layers of N26MT2Nb austenitic steel in which, due to elastic-plastic strain — the former strain induced martensite can be obtained by the abrasive paper grinding and shot penning. In this way the assessment of useful layers for the electro-spark nitriding can be established. Temperature and time of nitriding process were adjusted to the temperature of stability of strain induced martensite.

An additional goal of the research was to reveal new properties of the surface layers by an application of X-ray diffraction methods based on grazing incidence angle X-ray diffraction geometry (GID) [6, 7]. The benefits of application of GID geometry in quantitative phase analysis and residual macroscopic stress measurements in the surface layer of high nickel austenitic alloy are presented.

2. Investigated alloy

An austenitic alloy with Ni, Ti, Mo and Nb (see the chemical composition in table 1) after high temperature plastic deformation was cooled down slowly. Subsequently, the samples were homogenised for 2 hours at the temperature of 1100°C. The microstructure in this state consisted of large grains of 150-200 μm in diameter. This austenitic alloy without precipitation performs the ability to martensite phase transformation under some plastic deformation. The samples were subjected to a surface preparation treatment by grinding with abrasive paper no. 120#, polishing with Al_2O_3 particles in water and/or burnishing by steam of steel balls in diameter of 3 mm with the speed of 300 m/sec during 5 min. The aim of this surface preparation was mainly to get some degree of strain induced martensite (α') in the surface layer before following electro-spark nitriding.

The thermal stability of strain induced martensite (α') was examined at 70% deformed samples by heating to 800°C at the heating rate of 10°C/min and by isothermal annealing at 400°C during 4.5 hours. This 400°C was the lowest temperature for the nitriding process with electro-spark technique. The main nitriding conditions were established to be 450°C during 1 hour.

TABLE 1

Chemical composition of investigated alloy in atomic %, Fe — bal.

Symbol	Ni	Ti	Al	Mo	Nb	C	Si	Mn	S	P
N26T2MNb	26.0	2.15	0.04	1.15	0.11	0.02	0.11	0.17	0.009	0.007

3. Methods of surface layer analysis

The phase content and gradient-like distribution of residual stress in the near surface volume can be determined by using the standard X-ray diffraction methods (Bragg-Brentano geometry B-B) repeated for several wavelengths [9] or by using geometrical combination of tilts of incidence and diffracted X-ray beam elaborated by B o n a r s k i [10]. Methods based on classical B-B geometry proved to be unsuitable for the analysis of non-uniform states because the penetration depth of X- ray radiation varied significantly during the measurement [6, 7, 11]. As a result, the volume for which the measurement is performed is not well defined, and the interpretation of the results becomes complex.

Recently the diffraction methods based on the grazing incidence angle *X*-ray diffraction geometry (GID) were applied to phase analysis and elastic strain measurement. The approach to gradient-like phase and residual stress distribution analysis based on GID geometry are characterised by a small and constant incidence angle (α) and by different lengths and orientations of scattering vector [6, 7, 11]. Inclination of scattering vector for particular {hkl} depends on Bragg angle (θ) and on α angle

($\psi = \theta - \alpha$). With the change of the α incidence angle, thickness of the measured surface layer differs which makes possible a non-destructive scan through depth (Z) [6, 7]. For the investigated alloy, this relation was calculated for two wavelengths (see results in table 2). The diffraction patterns were recorded with D8-Advance diffrac-

TABLE 2

Comparison of calculated depth of penetration of X-ray beam for GID and BB diffraction geometry for λCoKα and λCuKα (G_x = 0.95% is fraction of the total diffracted intensity from the surface layer of Z thickness, Z was calculated for $\mu = 582.4cm^{-1}$ and $\mu = 1982.4cm^{-1}$ as linear absorption coefficients) [8]

Angle α [deg]	1	2	5	9	14	20	BB
Depth Z λCuKα [μm]	0.2	0.5	1.1-1.2	1.7-2	2-3	3- 4	0-7.5
Depth Z λCoKα [μm]	0.9	1.8	3.8-4.1	6-7	8-10	11- 14	0-26

tometer using λCoKα filtered wavelength, step-scanning mode with $\Delta 2\theta$ = 0.04 deg under GID and BB geometry (Fig.1-4).

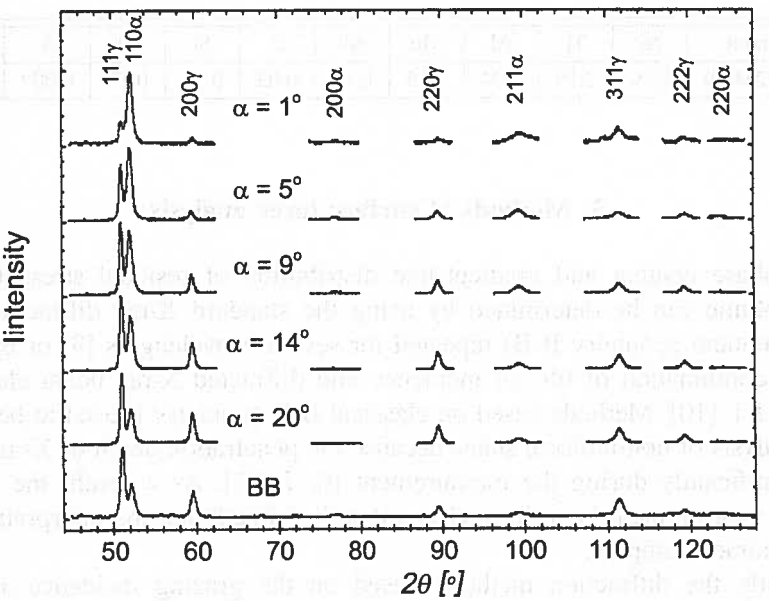

Fig. 1. Diffraction patterns for different thickness of surface layers and incidence angles α (see Tab. 2) of grazing angle X-ray diffraction and Bragg-Brentano (BB) geometry of ground samples

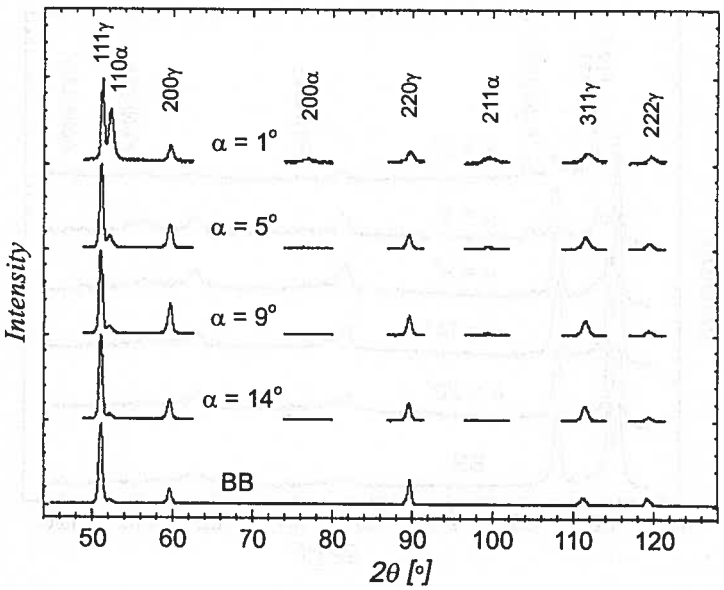

Fig. 2. Diffraction patterns for different thickness of surface layers and incidence angles α (see Tab. 2) of grazing angle X-ray diffraction and Bragg-Brentano geometry (BB) for polished samples

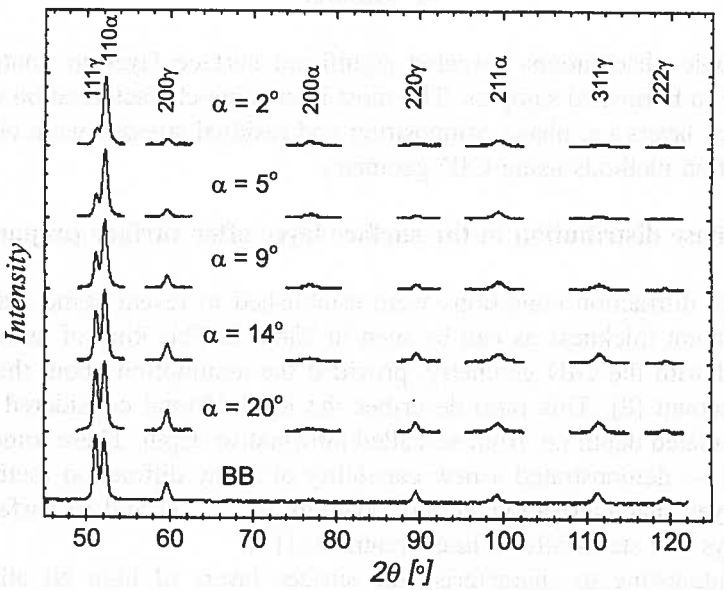

Fig. 3. Diffraction patterns for different thickness of surface layers and incidence angles α (see Tab. 2) of grazing angle X-ray diffraction and Bragg-Brentano (BB) geometry of burnished samples

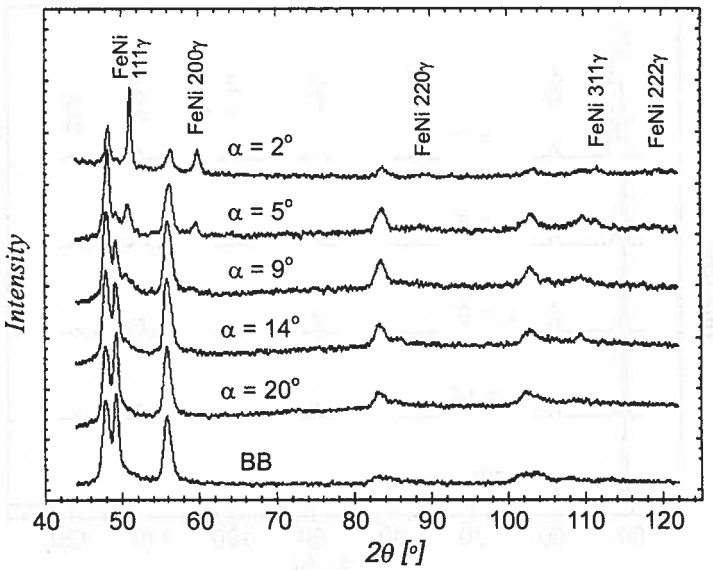

Fig. 4. Diffraction patterns of nitrided surface layers on burnished sample for different thickness and incidence angles α by means of GID and B-B diffraction geometry

4. Results

Microscopic observations revealed significant surface layer in contrast to bulk material only in burnished samples. The most interesting characterisation of the investigated surface layers i.e. phase composition and residual stresses were obtained with X-ray diffraction methods using GID geometry.

4.1. Phase distribution in the surface layer after surface preparation

The x-ray diffraction conditions were established to reveal some features of the layers of different thickness as can be seen in Table 2. This kind of examination can be performed with the GID geometry, provided the assumption about the G_x ratio is taken into account [8]. This ratio describes the level of total considered information from the calculated depth i.e. from so-called informative depth. These tomography-like examinations — demonstrated a new capability of X-ray diffraction methods applied to surface layer characterisation in TiN coatings [6, 7, 11] and to surface layers of titanium alloys and steels after a laser treatment [11].

It was interesting to characterise the surface layers of high Ni alloy after the mechanical preparation and thermo-chemical treatment. The analysis of diffraction patterns (Fig.1–4) using quantitative X-ray diffraction internal reference phase analysis enabled to reveal the distribution of phase content under the surface (Fig.5). The application of a modified $g = sin^2\psi$ method [6, 7, 11] allowed to get a new approach in measurement of residual macro-stresses distribution in a non-destructive way (Fig.6).

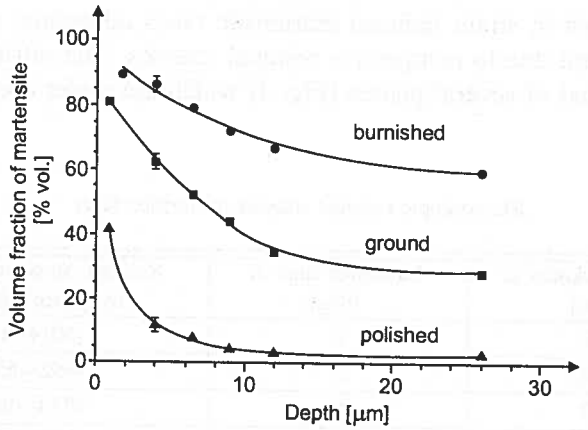

Fig. 5. Influence of surface preparation means on phase composition versus thickness of surface layer

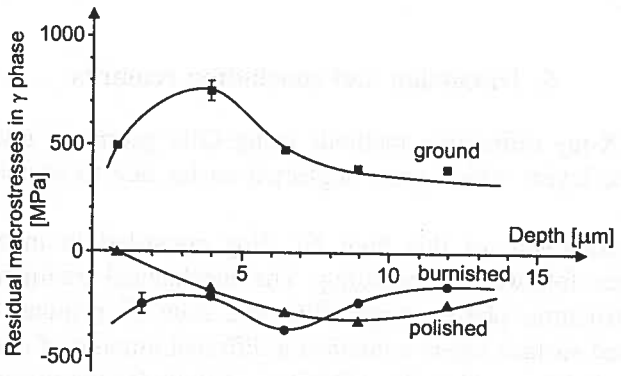

Fig. 6. Influence of surface preparation methods on residual stresses distribution versus thickness of surface layer

The samples ground with No.120 abrasive paper contained different quantities of α' martensite from 81% for a surface layer of 2 μm thickness to 24,5% for a surface layer of 26 μm thickness (see Figs.1 and 5), whereas the polished samples with the same thickness of surface layers contained from 41,2 vol.% to 4,3 vol.% of α' martensite, respectively (see Fig.2-5). The thin surface layers of the burnished samples contained almost pure α' martensite and the thickness of the surface layer with the transformed strain martensite was much larger (see Fig. 3 and 5).

4.2. Results of nitriding by electro-sparks mode on burnished samples

Surface layer and microstructure of burnished austenitic samples is characterised by the presence of strain martensite and compressive residual stresses. Both are connected with enhanced internal energy, which influences the diffusion of nitrogen. A larger

diffusion of nitrogen in strain induced martensite takes adventage in comperision to dumping of diffusion due to compresive residual stresses. The nitrided surface layers in this case consisted of several phases (Fig. 4) which are under compressive residual stresses (Tab.3).

TABLE 3

Macroscopic residual stresses in nitrided layer

Layer thickness Z [μm]	Incidence angle α [deg]	Residual stress in γ phase by $g-sin^2\psi$[MPa]
1.7	2	-601+-60
3.8-4.1	5	-652+-65
6-7	9	-1030+-103
8-10	14	-550+-55
11-14	20	-323+-32

5. Discussion and concluding remarks

The applied X-ray diffraction methods using GID geometry revealed fine structure of the surface layers which were neglected so far due to standard methodology limitations.

The surface treatment of this high Ni alloy consisted in mechanical preparation of the surface followed by nitriding. The mechanical treatment was to create a special microstructure, phase composition and state of residual stresses. Among others, the obtained surface layers contained a different amount of α'strain martensite. This structure created supporting (beneficial) conditions for the nitriding process. The maximum content of strain martensite approached 90 vol.% and its distribution was gradient-like decreasing along the thickness. The results obtained by grazing incidence angle X-ray-diffraction (figures 1-3, tables 3-5) concern a surface layer 1.7 to 14 μm thick. The results present average values, according to the rules of the diffraction methodology. The structural characteristics are gradient-like and they can increase diffusion of nitrogen atoms during successive thermo-chemical treatment.

The best results of nitriding appeared on burnished samples with large content of strain martensite and deformed austenite. This kind of surface layers derived an extra energy to enhance the diffusion of nitrogen.

6. Conclusions

The new methodological approach demonstrates that mechanical surface treatment of the austenitic N26MT2Nb alloy depends greatly on the properties of the surface layer and on the successive diffusion processes during electro-spark nitriding. The following conclusions can be formulated on the basis of the experiment described:

1. Grinding, polishing and burnishing produce different surface layers consisting of different amounts of austenite, strain martensite and different level of residual macrostresses. The thickness and structure of these surface layers are different and they reveal different properties in comparison with bulk alloy.

2. Dynamical burnishing of coarse grain N26MT2Nb austenitic alloy yields a surface layer of more than 30 μm in thickness with gradient-like distribution of austenite, strain martensite and compressive residual stresses.

3. The X-ray diffraction methods based on the grazing incidence angle X-ray-diffraction geometry demonstrate their new applicability to the characterisation of the surface layer.

Acknowledgements

The authors wish to acknowledge K.Chruściel, M. Sc. in the research project which was supported by the Polish Committee for Scientific Research — KBN under grant No. 4 T08C 018 25.

REFERENCES

[1] J. Jeleńkowski, Materials Science and Technology **10**, 1073 (1994).
[2] Yu. Zhiwej, Xu. Xiaolei, W. Liang, at all., Surface and Coatings Technology **153**, 125 (2002).
[3] A.I. Uvarov, T.P. Vasechkina, Phys. Met. Metallov. **4** .92 (2001).
[4] T. Burakowski, T. Wierzchoń, Inżynieria powierzchni metali. WNT Warszawa 1995.
[5] J. Jeleńkowski, K.J. Kurzydłowski, k. Rożniatowski, Inżynieria Materiałowa **6**, 505 (2003).
[6] S.J. Skrzypek, A. Baczmanski, *Adv. X-ray Anal.*, **44**, 134 (2001).
[7] S.J. Skrzypek, A. Baczmański, W. Ratuszek, E.J. Kusior, J. Appl. Cryst. **34**, 427 (2001).
[8] B.D. Cullity, S.R. Stock, Elements of X-Ray Diffraction, 3-rd edition, Prentice Hall Upper Saddle River, NJ 07458 2001.
[9] I. Kraus, N. Ganev, X-ray analysis of the inhomogeneous stress state, In: Defects and Microstructure Analysis by Diffraction, Eds. R.L.Snyder, J.Fiala and H.J.Bunge, Oxford University Press Inc., New York, 367-401 (1999).
[10] J.T. Bonarski, Rentgenowska tomografia teksturowa. Polska Akademia Nauk, Inst. Metalurgii i Inż. Materiałowej Kraków 2001.
[11] S.J. Skrzypek, Nowe możliwości pomiaru makro-naprężeń własnych w materiałach przy zastosowaniu dyfrakcji promieniowania X w geometrii stałego kąta padania, ROZPRAWY i MONOGRAFIE 108, Uczelniane Wyd. Nauk.-Dydaktyczne AGH, Kraków 2002.

Received: 24 January 2005.